



FACILITY FORM 502

NG5 - 24034
 (ACCESSION NUMBER)

47
 (PAGES)

CR-56698
 (NASA CR OR TMX OR AD NUMBER)

(THRU)

(CODE)

~~32~~ 32
 (CATEGORY)

GPO PRICE \$ _____

OTS PRICE(S) \$ _____

Hard copy (HC) \$ 2.00

Microfiche (MF) .50

ALLIED RESEARCH ASSOCIATES
 VIRGINIA ROAD CONCORD, MASSACHUSETTS

**DEVELOPMENT AND APPLICATION
OF BASIC ANALYTICAL PRINCIPLES
FOR MATERIALS AND DESIGN SYNTHESIS
TO ADVANCED CONCEPTS
FOR SPACE AND LAUNCH VEHICLES**

QUARTERLY PROGRESS REPORT NO. 268-1
MARCH 23, 1964 - JUNE 23, 1964

prepared for
CONTRACT NO. NASw-928
NATIONAL AERONAUTICS AND SPACE ADMINISTRATION
WASHINGTON 25, D. C.

ALLIED RESEARCH ASSOCIATES, INC.
VIRGINIA ROAD CONCORD MASSACHUSETTS

DEVELOPMENT AND APPLICATION OF BASIC ANALYTICAL PRINCIPLES FOR MATERIALS AND DESIGN SYNTHESIS TO ADVANCED CONCEPTS FOR SPACE AND LAUNCH VEHICLES

Introduction

During the first quarter of this contract, our major research effort was conducted in the area of energy absorbing structures/materials for spacecraft landing systems. In addition, an effort was initiated on the synthesis implications of the statistical aspects of structural design with particular regard to shell buckling problems and the use of high strength, low ductility materials in pressure vessels.

Spacecraft Landing Systems

Our previous design synthesis work under Contract No. NASw-682 identified high strength-weight ratio of solid materials as an important parameter in achieving efficient spacecraft landing systems. Since such materials are generally in compression, they are subject to various buckling modes and, therefore, their strength-weight ratio depends upon the structural configuration as well as the material selected.

The progress report included herein entitled "Spacecraft Landing Systems: Preliminary Design Considerations Utilizing Plastically Buckled Tubes as Energy Absorbers" presents the basic analytical principles for a potentially efficient landing system which limits the maximum deceleration and deceleration onset rate to the prescribed parametric values obtained from the design synthesis study and presented in Ref. 2 of the appended report. In all cases, the deceleration limiter and onset limiter combinations have been optimized for minimum weight.

In addition to the information presented in the appended report, we have conducted studies during the past quarter on the design synthesis of other forms of energy absorbers such as gas bags and retrorockets. These studies are in parametric form and serve to identify the structures, materials and design indices of fundamental importance in establishing the relative efficiencies of the various competitive approaches.

It is planned to complete this design synthesis during the next quarter in the form of a summary report.

Statistical Aspects of Structural Design

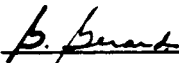
During the past decade, emphasis on reliability predictions of structural designs has served to introduce statistical methods in an ever expanding role in the structures field. Statistical methods are of particular importance in at least two major areas of concern under our present contract: buckling of shells and the use of high strength, low ductility materials for pressure vessels. In both cases the inherent scatter of the test results indicate that statistical methods probably should be incorporated into the design synthesis of such structural components.

Accordingly, we have initiated a critical literature review of this field during the past quarter and plan to utilize the current state-of-the-art in our design synthesis studies during the next quarter.

Pressure Vessels

During the next quarter, we also plan to initiate an effort concerned with the design synthesis of pressure vessels. Since pressure vessels are designed on the basis of tensile strength in the presence of structural and fabrication stress concentration factors, the synthesis will include such factors.

It is planned that this study will be sufficiently comprehensive to include pressure vessel configuration and stabilization and the influence of combined internal pressure and axial compressive loading requirements upon the design synthesis.



George Gerard

Project Manager

**SPACECRAFT LANDING SYSTEMS:
PRELIMINARY DESIGN CONSIDERATIONS
UTILIZING PLASTICALLY BUCKLED
TUBES AS ENERGY ABSORBERS**

**ROGER MILLIGAN
JUNE 19, 1964**

**prepared for
CONTRACT NO. NASw-928
NATIONAL AERONAUTICS AND SPACE ADMINISTRATION
WASHINGTON 25, D. C.**

**A L L I E D R E S E A R C H A S S O C I A T E S , I N C .
VIRGINIA ROAD CONCORD MASSACHUSETTS**

ABSTRACT

24034

Two concepts are proposed for utilizing solid structural materials as efficient energy absorbers. It is suggested that the maximum deceleration of a landing vehicle can be controlled by utilizing a landing system design wherein a structural element in the form of a cylindrical shell is designed to deform via the axisymmetric buckling mode. The rate of change of deceleration of the vehicle would be limited by a second structural element in the form of a tapered shell designed to deform plastically at the operating stress. It is postulated that these two basic energy absorbing elements, the deceleration limiter and onset rate limiter, when incorporated in a landing system design would provide vehicle deceleration characteristics similar to that of an ideal energy absorber.

Analytical techniques are developed such that a detailed design configuration for these energy absorbing elements can be determined based on gross vehicle and landing system design parameters. Test results are presented for axisymmetric buckled tubes which support the design hypothesis.

Author

TABLE OF CONTENTS

	<u>Page</u>
ABSTRACT	v
LIST OF ILLUSTRATIONS	vii
LIST OF SYMBOLS	viii
1. INTRODUCTION	1
2. GENERAL DESIGN PROCEDURE	6
Performance Relationships	6
Weight Considerations	6
Optimum Peak Deceleration Factor	10
Deceleration Limiter Configuration	14
Onset Limiter Configuration	20
3. DISCUSSION	30
4. CONCLUSION AND RECOMMENDATIONS	36
REFERENCES	37

LIST OF ILLUSTRATIONS

<u>Figure No.</u>		<u>Page</u>
1	Vehicle Deceleration Time History with a Landing System Employing an Ideal Energy Absorber	2
2	Energy Dissipating Systems	7
3	Optimum Design Peak Deceleration Factor as Determined by Vehicle Landing Energy Absorption Requirements and Landing System Structural Stability Considerations	9
4	Representative Curves which Give the Optimum Peak Deceleration Factor for a Particular Vehicle Landing Configuration and Landing System Design Configuration	13
5	Optimum Peak Deceleration Factor Versus Vehicle Landing Parameter and Landing System Design Parameters	15
6	Axisymmetric Buckling Stress Versus Cylinder Geometry	18
7	Curve of Functional Relationship Between Two Landing System Design Parameters	22
8	Onset Limiter Cross Sectional Area vs Stroke	23
9	Onset Limiter Cone Wall Thickness Versus Stroke	25
10	Buckling Correction Factor, C, for Cylinders or Cones	27
11	Cone Buckling Stress vs Geometry	28
12	Representative Load - Deflection Curve for a Cylinder Designed to Deform via the Axisymmetric Buckling Mode	32
13	Cylindrical Test Specimens Deformed Under Axial Compressive Loading via Axisymmetric Buckling Mode	33

SYMBOLS

A	cross sectional area (in. ²)
A ₁	cross sectional area of energy absorbing material associated with the end of stroke (in. ²)
\bar{A}	nondimensional cross sectional area
C	cone buckling coefficient
E	Young's modulus (psi)
E _s	secant modulus (psi)
E _t	tangent modulus (psi)
g	planetary acceleration due to gravity (in/sec ²)
h	wall thickness (in)
h _o	wall thickness associated with end of stroke (in)
\bar{h}	nondimensional wall thickness
I	area moment of inertia (in ⁴)
k _x	buckling coefficient
L	length (in)
N	number of landing struts absorbing vehicle impact loading
N _x	cylinder buckling load (pounds per inch)
n _o	peak deceleration factor
P	landing strut load (pounds)
P _{cr}	peak buckling load (pounds)
R	cylinder radius, maximum cone radius (in)
r	cone radius (in)
t ₁	time associated with end of stroke (sec)
V _i	vehicle touchdown velocity (in/sec)
W _v	vehicle gross weight (pounds)

SYMBOLS (contd)

x	vehicle displacement after touchdown as a function of time, landing system stroke, axial deflection (in)
x_c	maximum stroke for composite energy absorber (in)
x_g	maximum stroke for onset limiter (in)
x_g	maximum stroke for deceleration limiter (in)
\bar{x}	nondimensional stroke
$\dot{\bar{x}}$	onset rate/g (sec^{-1})
Z	= L^2/Rh
α	cone apex half angle
β	= $n_o V_i / (x_c \ddot{x})$
δ	= $(g/V_i^2) (W_v/N)^{1/2}$ (pounds per inch)
η	plasticity reduction factor
λ	= $n_o^2 g / (V_i \ddot{x})$
ν	Poisson's ratio
ν_e	elastic value of Poisson's ratio
ζ	= $V_i / (x_c \ddot{x})$
ρ	radius of gyration (in)
σ_c	buckling stress in primary column mode (psi)
σ_{cr}	local buckling stress (psi)
σ_{cr_e}	elastic local buckling stress (psi)
ϕ	= $\pi^3 E_t (h/R)(R/L)^4$ (psi)

SUBSCRIPTS

g	deceleration limiter
\dot{g}	onset limiter

1. INTRODUCTION

One of the objectives of the U. S. space program is to obtain environmental data from scientific instrumentation placed on planetary surfaces. To implement this goal, it is necessary to design impact energy absorption systems which will allow a soft landing capability for space vehicle payloads. Such systems must not only attenuate vehicle landing motions in a manner compatible with payload fragility but also be designed for minimum weight and maximum reliability.

A recent survey of energy absorption techniques (Ref. 1) reveals that energy absorbers using structural materials show considerable promise for space vehicle applications. For example, structural material energy absorbers in many cases have a larger energy absorbing efficiency than systems using gas bags or braking rockets. In addition, these materials can be incorporated in a design which affords maximum simplicity of operation and attendant high reliability. They also can be designed to arrest vehicle motion with a minimum of rebound which is another desirable landing system characteristic.

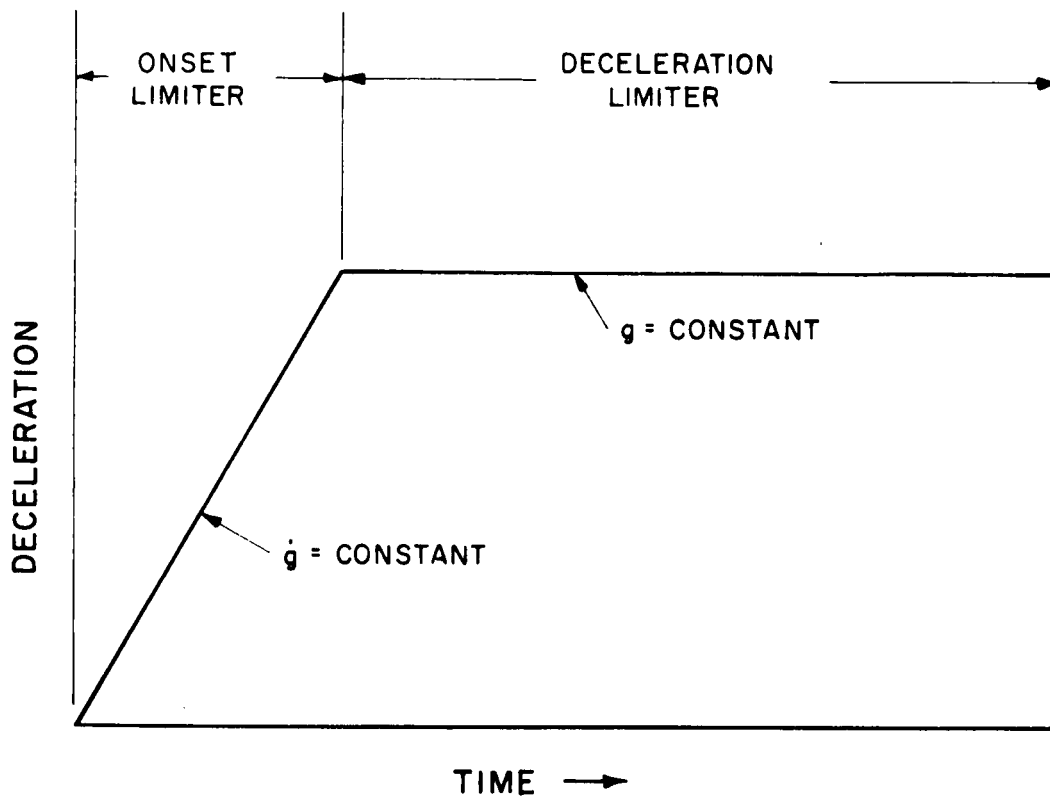
In order to assess the relative merit of present generation energy absorbers using structural materials, it is desirable to review factors affecting the performance and weight of landing system design.

As noted above, payload fragility is an important consideration in landing system design. Payload fragility can be described in terms of allowable onset rate and peak deceleration. Hence, an essential feature of the performance of any landing system design is that it exercise control over vehicle landing motions compatible with these payload restrictions. A landing system design using an ideal energy absorber would result in a vehicle deceleration time history as shown in Figure 1. One observes from this figure that the vehicle deceleration increases linearly (the onset rate is constant) to a maximum value and then remains constant (zero onset rate) until vehicle motion is arrested. In the development which follows it is convenient to consider the deceleration - time profile of Figure 1 to consist of two regions, an onset limiter region (constant onset rate) and deceleration limiter region (constant deceleration) as shown. For maximum landing system efficiency, i.e., minimum weight and stroke, the onset rate and peak deceleration imposed on the vehicle by the landing system would equal the maximum values which could be tolerated by the payload.

In Ref. 2, an analysis was made of the weight of a landing system using an

FIG. 1

VEHICLE DECELERATION TIME HISTORY WITH A LANDING SYSTEM EMPLOYING AN IDEAL ENERGY ABSORBER



ideal energy absorber and associated vehicle deceleration characteristics as indicated by Figure 1. It was shown that for landing systems using solid materials, weight considerations favor designs with a high material efficiency (operating stress to material density ratio) and a high stroke to length ratio of the solid material before bottoming occurs.

Some of the proposed design techniques which use structural materials as energy absorbers include honeycomb structures, elastic collapse tubes, collapsible struts, and the frangible tube. Although all of these approaches represent relatively efficient energy dissipation, problems of landing system design particularly with regard to the control of the onset rate have not been fully explored. It also appears that improvements in the efficiency of structural materials can be realized through advanced design techniques.

For certain energy absorbers using structural materials, the working stress associated with material deformation is relatively low; hence, the corresponding material and energy absorbing efficiency for such designs is penalized. For example, honeycomb structures are usually designed such that core buckling stress which initiates crushing of the cells is in the elastic range of the material. Similarly, deformation of the collapsible tube of Ref. 3, is predicted on an asymmetric buckle pattern which is induced at relatively low elastic stress levels. In the collapsible strut (Ref. 4) and frangible tube designs (Ref. 5), high material efficiencies are obtained by utilizing the inelastic or plastic regime of the material as the working stress. For the collapsible strut, however, material deformation associated with energy absorption is confined to a relatively small portion of the total structure located at the strut elbow; hence, the full energy absorbing capability of the construction material is not developed. In the frangible tube design, working stresses associated with material rupture are developed throughout the working stroke. However, this technique requires a relatively heavy die to provide an anvil for shreading the frangible tube. It is noted that the problem of controlling the onset rate has not been considered in detail for any of the aforementioned designs.

Consideration of those factors which contribute directly to energy absorption efficiency (high material efficiency and high stroke to length ratio) has led to a novel design technique for dissipating impact energy. It is postulated that a cylindrical tube designed to deform via an axisymmetric buckling mode will provide a constant force in resistance to shell deformation throughout its stroke. This behavior when incorporated in a landing system design would produce vehicle deceleration

characteristics similar to that shown by the "deceleration limiter" range of Figure 1.

The theoretical groundwork for the design of a tube which will buckle in an axisymmetric mode has already been established in Ref. 6. Data presented in Ref. 6 show that the theory is in excellent agreement with experimental results, particularly for design buckling stresses approaching or exceeding the material yield strength. It is apparent, therefore, that cylinders designed to buckle in the axisymmetric mode will realize a maximum value of the material efficiency parameter for materials in compression. Since the wavelength of the axisymmetric buckle pattern is small, a large portion of the tube following inception of the initial buckle will be undeformed and available for further energy dissipation. Continued application of compression loading would induce additional buckles along the tube length. Again, due to the small buckle size, a large portion of the tube should be developed as working stroke. This design technique, therefore, has the potential for a high material efficiency and a large stroke to length ratio which characterizes an efficient energy absorber.

As demonstrated in Ref. 7, shaped crushable structures can be designed to control the onset rate associated with arresting the motion of a free falling mass. In this application, the energy absorbing material is distributed in the form of a cone or pyramid. The force generated by the crushable structure in resisting motion is therefore developed gradually, and the corresponding deceleration is controlled.

The energy absorbing material utilized in Ref. 7 was aluminum honeycomb which due to its low solidity has a relatively low average operating stress associated with elastic buckling. More efficient energy absorption could obviously be obtained if solid materials could be designed to flow plastically at stresses approaching the material yield. It is postulated, therefore, that an efficient energy absorbing structure of the onset limiter type could be obtained by distributing material in a tapered configuration such that each cross section of the element works to the yield stress when absorbing impact energy. It is noted that materials with the highest yield stress to density ratio will provide the most efficient energy absorption.

In summary, two design concepts have evolved for attaining an efficient impact energy absorber for landing systems. First, it is proposed that a tube designed to deform via axisymmetric buckling when incorporated in a landing system design will provide efficient energy absorption and control the peak vehicle deceleration. Secondly, it is suggested that solid structural materials can be shaped in cross section and integrated in landing system design so as to provide efficient impact

energy absorption and also control the vehicle rate of change of deceleration. The combination of the deceleration and onset limiting elements should provide vehicle deceleration characteristics similar to that of the ideal energy absorber shown in Figure 1.

In the subsequent development, the design considerations examined are associated with the use of shell-type structures for energy absorbers based on the concepts enumerated above. In addition, a general design procedure is developed which integrates the detailed design of the energy absorbing element and the vehicle gross landing and configuration parameters.

2. GENERAL DESIGN PROCEDURE

Performance Relationships

As postulated in the Introduction, the characteristics of a thin walled cylinder designed to deform under axial compression via an axisymmetric buckling mode will be similar to that of a deceleration limiter -- i.e., the tube will provide a force resisting deformation which is essentially constant with stroke and time. In addition it is suggested that energy absorption similar to that of an onset limiter can be obtained by proportioning a shell such that the force resisting deformation is developed gradually. Based on this hypothesis, vehicle deceleration characteristics for a landing system which incorporates such elements would be as shown in Figure 1.

The performance of this ideal type of energy absorber has been determined in Ref. 2 and is summarized by the following equations.

$$x_c = (V_i^2 / n_o g) [1/2 + \lambda/2 - \lambda^2/24] \quad (1)$$

$$x_{\dot{g}} = (V_i^2 / n_o g) [\lambda - \lambda^2/6] \quad (2)$$

$$x_g = (V_i^2 / n_o g) [1/2 - \lambda/2 + \lambda^2/8] \quad (3)$$

$$\beta = n_o V_i / (x_c \ddot{x}) = [1/2 - \lambda/24 + 1/(2\lambda)]^{-1} \quad (4)$$

where $\lambda = n_o^2 g / V_i \ddot{x}$

These equations are based on the assumption that the change in potential energy of the vehicle associated with deformation of the landing system is negligible compared to the vehicle touchdown kinetic energy.

Weight Considerations

Possible techniques for dissipating landing impact energy via an onset limiter, deceleration limiter, or composite (deceleration and onset limiter) system are illustrated schematically in Figure 2. All curves represent the same total energy dissipated. As indicated, curve "A" is for a landing system using a deceleration limiter only, curve "B" is for an onset limiter only, and curves "C" and "D" apply to a landing system with a composite energy absorber -- i.e., composed of both onset and deceleration limiting elements. The disadvantages of the systems using either onset limiters or deceleration limiters (curves "A" and "B") are readily apparent. The deceleration limiter design exceeds the allowable onset rate whereas

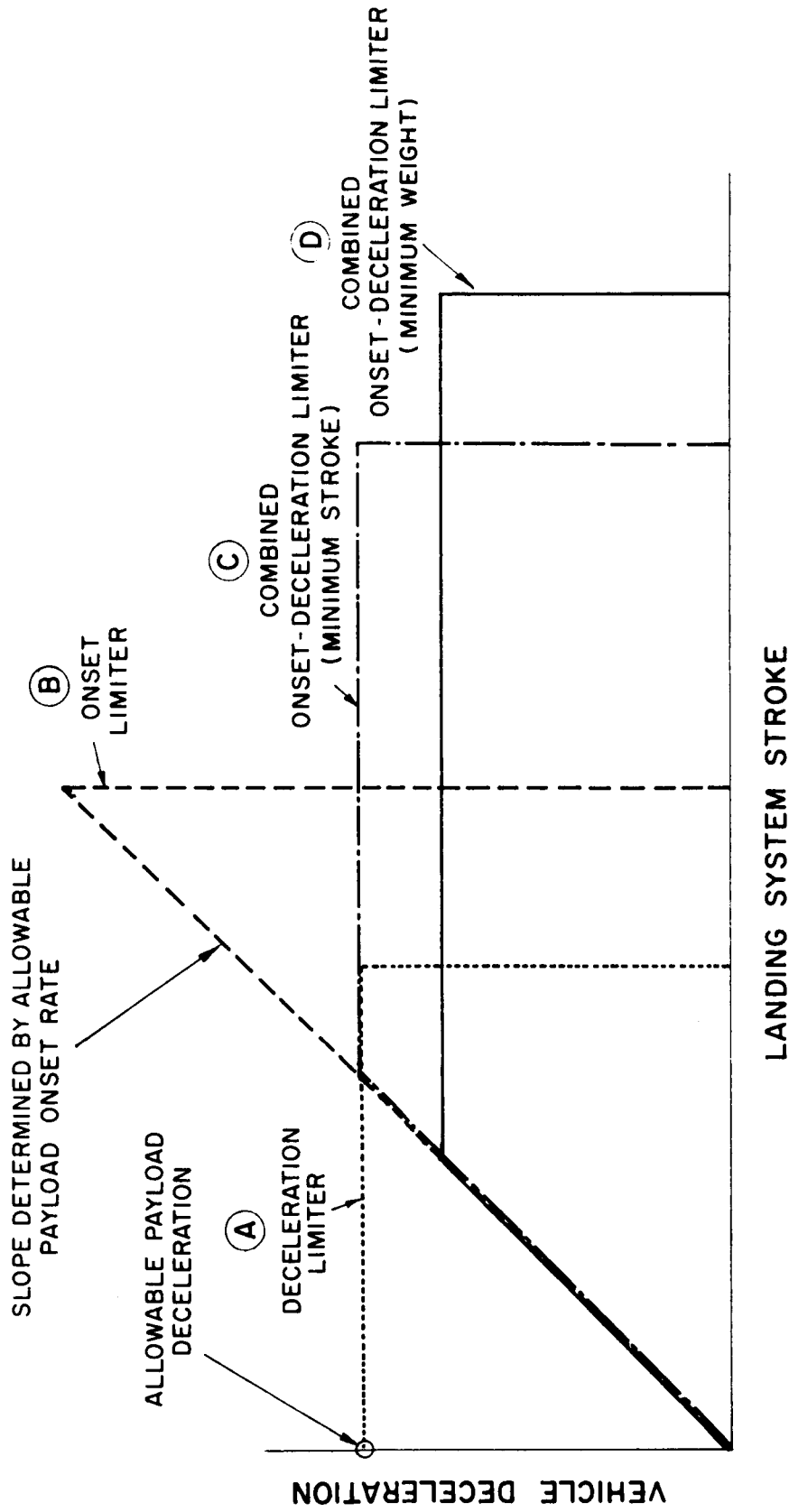


FIG. 2

ENERGY DISSIPATING SYSTEMS

the onset limiter design exceeds the allowable peak deceleration as determined by payload fragility. Intuitively one would expect that the composite energy absorber which develops the full allowable onset rate and peak deceleration as determined by payload fragility (curve "C") would represent a minimum weight design. However, for energy absorbers using solid materials whose stroke to length ratio is less than unity, it was shown in Ref. 2 that the deceleration limiter has a greater efficiency than the onset limiter. Minimum weight considerations, therefore, favor designs wherein a larger portion of the total impact energy is dissipated via the deceleration limiter technique. For this reason, curve "D" of Figure 2 represents a minimum weight design as compared with curve "C".

One observes from a comparison of curves "C" and "D" of Figure 2 that the stroke of the deceleration limiting region of operation increases as the peak deceleration of the vehicle decreases. A maximum design value for this stroke is determined by the length for which the deceleration limiter buckles as a column. This consideration is illustrated schematically by Figure 3. Curve "E" of this figure depicts the increase in deceleration limiter stroke associated with a decrease in peak deceleration factor and is determined by energy absorption requirements. Curve "F" shows that the allowable column length decreases as the peak deceleration factor decreases. The intersection of these two curves gives the maximum permissible stroke and the associated minimum value of the deceleration factor. For peak deceleration factors less than the minimum value, the stroke required to dissipate landing energy would exceed the critical column length for the deceleration limiter, and the landing system would fail via a general instability mode instead of in the desired local instability mode. Since the minimum peak deceleration represents a minimum landing system weight as described above, the minimum deceleration factor corresponds to the optimum design condition. It is noted that the curves shown in Figure 3 represent a particular vehicle gross weight, touchdown velocity, and onset rate condition.

The above considerations for determining the optimum peak deceleration factors are based on theoretical results which show that the deceleration limiter is a more efficient energy absorber than the onset limiter. If the application of design techniques result in an energy absorber wherein the converse is true -- i.e., the onset limiter is the most efficient element, then the optimum peak deceleration factor would correspond to the maximum or the allowable deceleration factor. For this case, the minimum weight landing configuration would also correspond to a minimum stroke configuration.

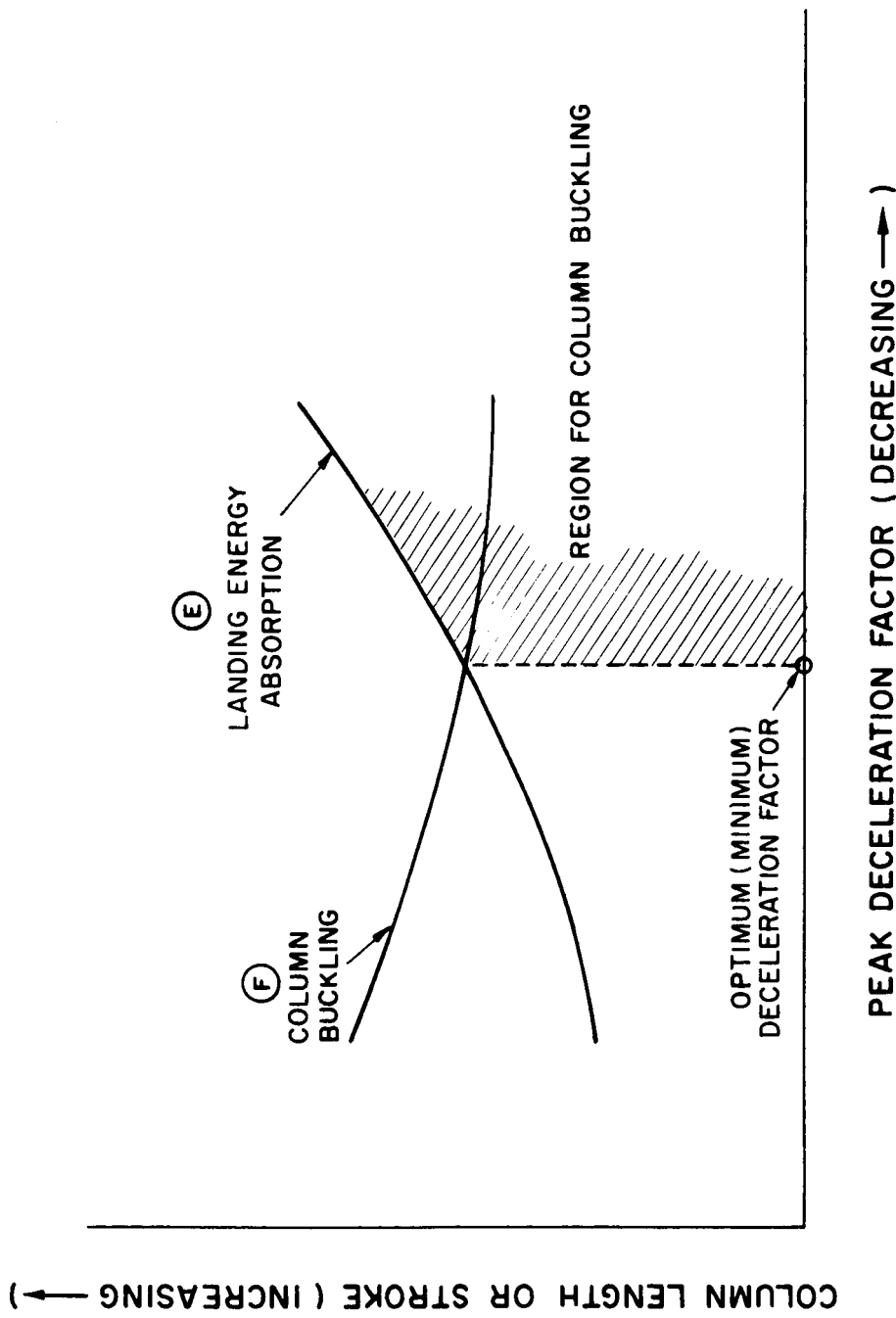


FIG. 3

**OPTIMUM DESIGN PEAK DECELERATION FACTOR AS DETERMINED BY
VEHICLE LANDING ENERGY ABSORPTION REQUIREMENTS AND LANDING SYSTEM
STRUCTURAL STABILITY CONSIDERATIONS**

Optimum Peak Deceleration Factor

For design purposes it is desirable to develop the relationships which determine the optimum peak deceleration factor such that this factor can be readily ascertained for all combinations of vehicle gross weight, touchdown velocity, and design conditions. For this reason, a procedure is presented below for determining the optimum peak deceleration factor in terms of generalized parameters. The method is developed as outlined under "Weight Considerations" above and is accomplished in three steps. First, energy absorption requirements are used to determine a relationship between deceleration limiter stroke, deceleration factor, and other design conditions. Secondly, from buckling considerations, the critical column length for the deceleration limiter is expressed as a function of deceleration factor and the vehicle and landing system configuration. Thirdly, the two relationships between stroke, critical column length, and deceleration are solved for the optimum deceleration factor. The final results are presented as a curve of optimum deceleration factor versus vehicle and landing system configuration parameters.

The energy absorption requirements for the landing system are implicit in the performance equations presented previously. Through use of the nondimensional stroke (Eq. 4), the peak deceleration factor may be expressed as follows:

$$n_o = \zeta^{-1} \left\{ 1/2 - \lambda/24 + 1/(2\lambda) \right\}^{-1} \quad (5)$$

where $\zeta = V_1 / (x_c \ddot{x})$

As indicated by Equation (5), for a given value of the design parameter ζ , the peak deceleration factor is a function of the parameter λ . The ratio of the stroke of the deceleration limiter to the total stroke is also a function of λ and from Equations (1) and (3) is

$$x_g/x_c = (1/2 - \lambda/2 + \lambda^2/8) / (1/2 + \lambda/2 - \lambda^2/24) \quad (6)$$

The ratio of the total length of the deceleration limiter to total working stroke can now be expressed as

$$L_g/x_c = (L_g/x_g)(x_g/x_c) \quad (7)$$

Substitution of Equation (6) in (7) gives

$$L_g/x_c = (L_g/x_g) \left[(1/2 - \lambda/2 + \lambda^2/8) / (1/2 + \lambda/2 - \lambda^2/24) \right] \quad (8)$$

For a given value of the parameter ζ , Equations (5) and (8) are both functions of λ , and through these equations the length ratio L_g/x_c can be graphed as a function of the peak deceleration factor. In this manner, energy considerations fix the length of the deceleration limiter as a function of peak deceleration (for a given ζ).

The buckling stress for a simply supported column subject to compressive axial loading (Ref. 8) is

$$\sigma_c = \pi^2 E_t / (L/\rho)^2 \quad (9)$$

where
$$\rho = (I/A)^{\frac{1}{2}} \quad (10)$$

Substitution of Equation (10) in (9) and rearranging terms gives

$$\sigma_c A = \pi^2 E_t I / L^2 \quad (11)$$

The product $\sigma_c A$ is the load carried by the structure at column buckling.

For a thin walled tube, the moment of inertia is given by

$$I = \pi h R^3 \quad (12)$$

Substituting Equation (12) in (11) and rearranging terms, one obtains

$$\sigma_c A = \pi^3 E_t (h/R) (R/L)^4 L^2 = \phi L^2 \quad (13)$$

where
$$\phi = \pi^3 E_t (h/R) (R/L)^4$$

Equation (13) expressing the column buckling load as a function of the column length and the material and geometry parameter ϕ .

If it is assumed that the vehicle payload has several landing struts and that the landing load is equally divided between the vehicle supports, the load per strut is

$$P = \sigma_c A = n_o W_v / N \quad (14)$$

For optimum design, the maximum load on the deceleration limiter strut will equal the column buckling load. Hence, from Equations (13) and (14), and introducing the stroke parameter x_c , the following relationship is determined

$$n_o W_v / N = \phi (L_g/x_c)^2 x_c^2 \quad (15)$$

or

$$(L_g/x_c)^2 = (1/\phi)(W_v/N)(n_o/x_c^2) \quad (16)$$

The total landing system stroke, x_c , is given by Equation (1) which allows Equation (16) to be written in the following form

$$(L_g/x_c)^2 = (\delta^2/\phi)[n_o^3/(1/2 + \lambda/2 - \lambda^2/24)^2] \quad (17)$$

where
$$\delta = (g/V_i^2)(W_v/N)^{\frac{1}{2}}$$

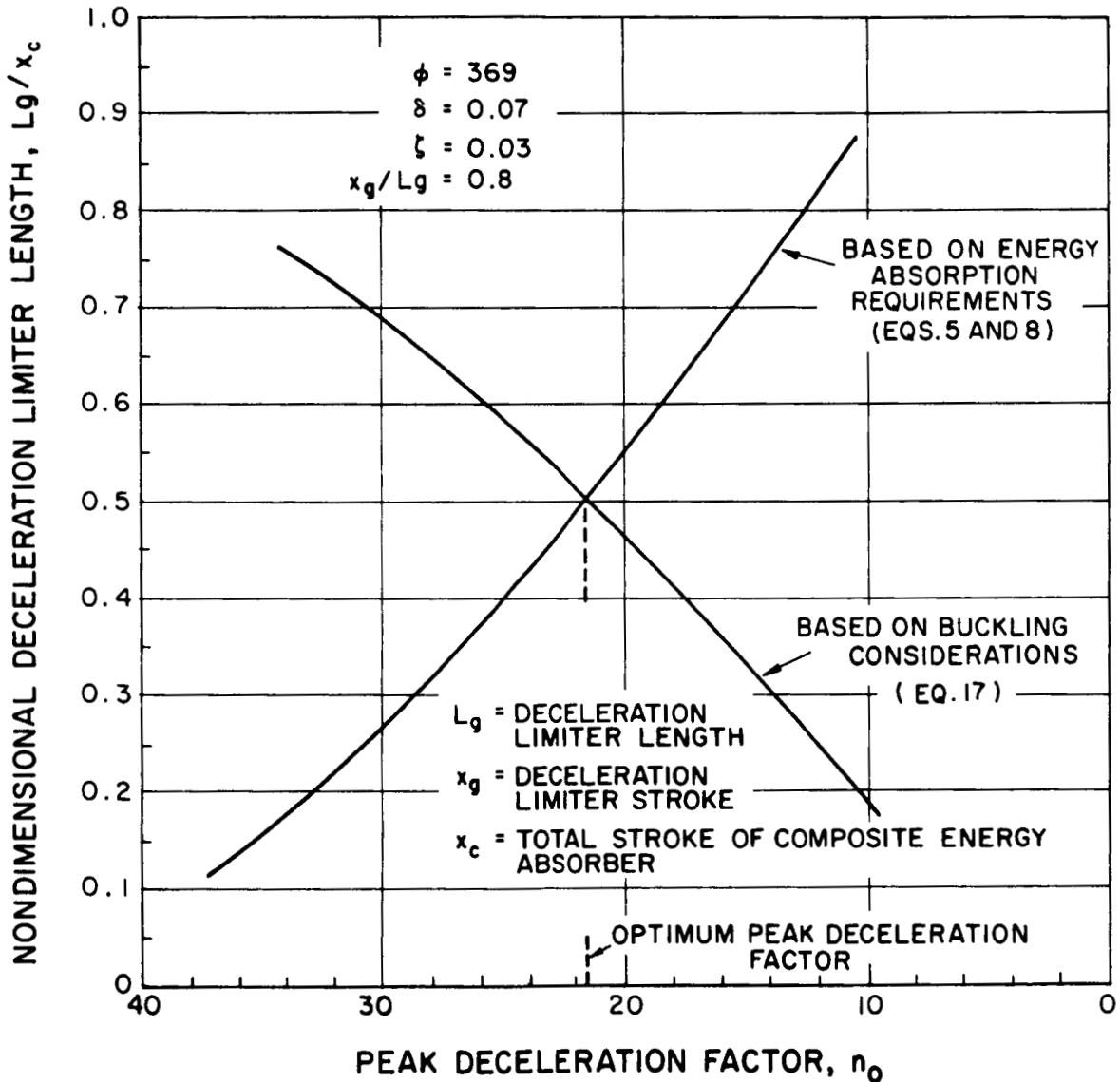
Equation (17) expresses the deceleration limiter to total stroke ratio as a function of the deceleration limiter material and geometry parameter ϕ , the vehicle landing configuration parameter δ , the design parameter λ , and the peak deceleration. It is noted that for a given value of the design parameter ζ , the peak deceleration factor and λ are not mutually independent but are related through Equation (5).

Equation (17) defines the deceleration limiter length ratio as a function of peak deceleration and was determined by buckling considerations. This ratio was also related to peak deceleration based on energy considerations and is given by Equations (5) and (8). A representative graph of these relationships is shown in Figure 4. As indicated, the curves were determined for a design parameter (ζ) of 0.03 and a vehicle landing configuration parameter (δ) of 0.07 lbs/in. These values correspond to a five thousand pound vehicle landing on earth with three landing struts, a sinking speed of approximately forty feet per second, a design energy absorber working stroke of approximately twenty inches, a stroke to length ratio of 0.8, and an allowable onset rate of eight hundred g's/sec. The deceleration limiter configuration parameter (ϕ) chosen for the illustration is 369. This value corresponds to a 7075-T6 aluminum cylinder with a radius/wall thickness ratio of 20.5, length radius ratio of eight, and design stress of 77,000 psi. Methods for determining these deceleration limiter parameters are presented in a subsequent subsection. One observes from Figure 4 that the optimum peak deceleration factor for the conditions assumed is 21.5.

Curves similar to Figure 4 could be prepared for other values of the parameters ζ and δ , and the corresponding optimum deceleration factor determined. However, a more direct method for obtaining the optimum peak deceleration factor as a function of vehicle parameters results by solving Equations (8) and (17) simultaneously. In this manner, the vehicle landing configuration parameter is found to be related to the peak deceleration factor and other parameters as follows

FIG. 4

REPRESENTATIVE CURVES WHICH GIVE THE OPTIMUM PEAK DECELERATION FACTOR FOR A PARTICULAR VEHICLE LANDING CONFIGURATION AND LANDING SYSTEM DESIGN CONFIGURATION



$$\delta = (L_g/x_g)(\phi^2)(1/2 - \lambda/2 + \lambda^2/8) n_o^{-1.5} \quad (18)$$

Again it is noted that λ and n_o are not independent but are related through the parameter ζ as given by Equation (5).

For prescribed values of the parameters, L_g/x_g , ϕ , and ζ , Equations (5) and (18) allow the vehicle landing configuration parameter to be determined as a function of the optimum peak deceleration factor. The results are presented as the curves of Figure 5. The abscissa of Figure 5 is the optimum deceleration factor, and the ordinate is the vehicle landing configuration parameter. One observes that for a fixed value of ζ , the optimum peak deceleration factor increases as the value of the vehicle landing parameter decreases. The curves shown are arbitrarily bounded by two lines which correspond to deceleration limiter length to total working stroke ratios of 0.125 and 0.89.

Through use of Figure 5, the optimum peak deceleration factor can be readily determined for any given value of the vehicle landing configuration parameter δ and design parameter ζ . It is noted that this figure applies only for a deceleration limiter configuration with a stroke to length ratio of 0.8 and a material and geometry parameter of 369. This latter value corresponds to a design in 7075-T6 aluminum as discussed above. Similar curves could be prepared for other deceleration limiter materials of construction and geometry.

Deceleration Limiter Configuration

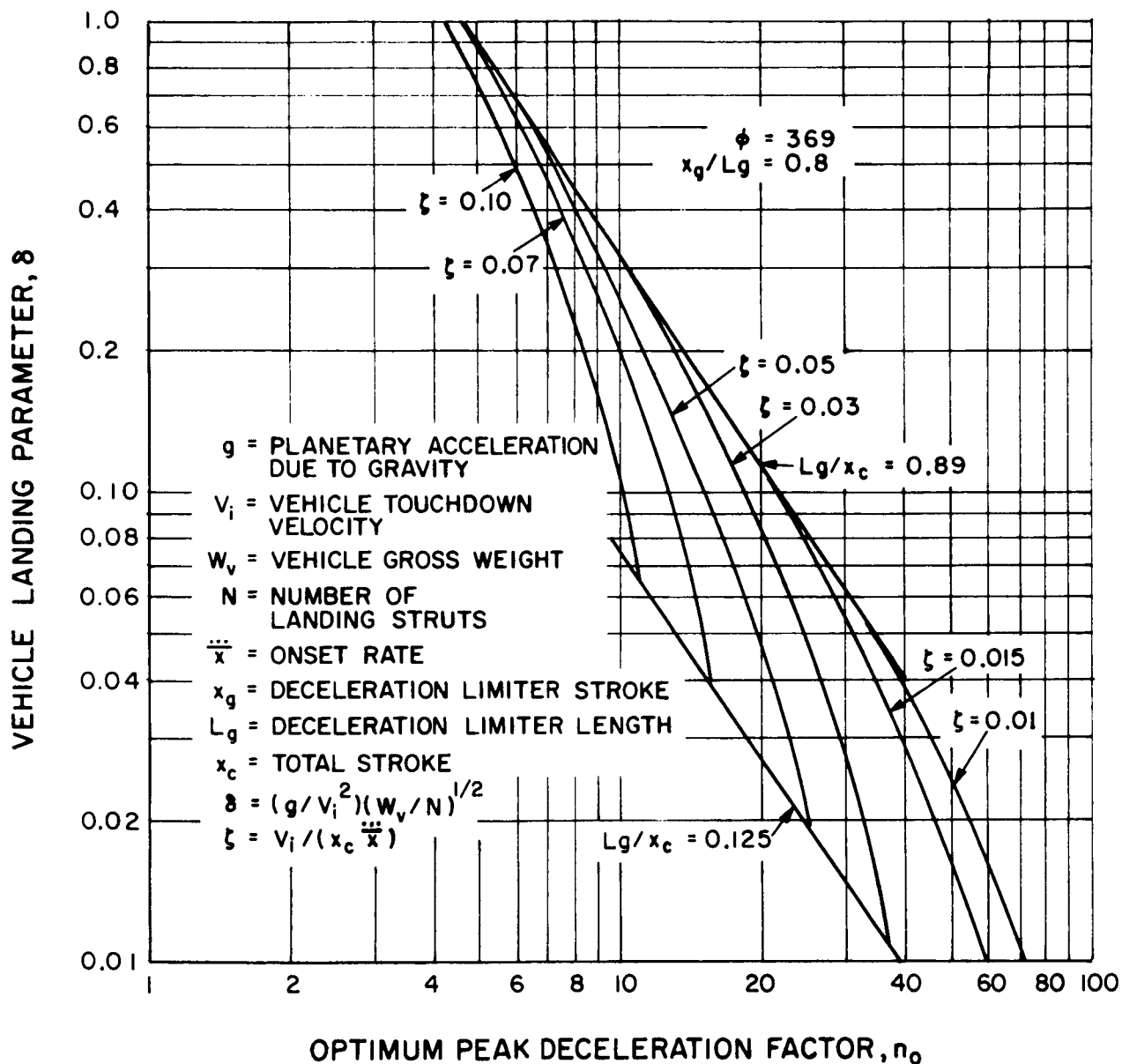
For this study, the deceleration limiting element of the landing design is a thin walled tube designed to deform via an axisymmetric buckling mode. The parameters which define the configuration are the tube radius to wall thickness ratio, the tube length to radius ratio, the wall thickness, and the material of construction. Presented below are general methods which allow the determination of these parameters. It is shown that for a given material the axisymmetric buckling criterion is satisfied by proper selection of the radius to wall thickness ratio; however, column buckling considerations dictate the appropriate length to radius ratio. The tube wall thickness follows from considerations of the total load which must be developed by the landing system to absorb vehicle impact energy.

As given in Ref. 6, the plastic buckling load for an isotropic cylinder is as follows:

$$N_x = \pi^2 \eta k_x EI / [(1 - \nu_e^2) L^2] \quad (19)$$

FIG. 5

OPTIMUM PEAK DECELERATION FACTOR VERSUS VEHICLE LANDING PARAMETER AND LANDING SYSTEM DESIGN PARAMETERS



For axisymmetric buckling, the plasticity reduction factor from Ref. 6 is

$$\eta = [(1 - \nu_e^2)/(1 - \nu^2)] (E_s/E)(E_t/E_s)^{\frac{1}{2}} \quad (20)$$

The equations for Poisson's ratio including plasticity effects (Ref. 9) and the elastic buckling coefficient (Ref. 6) are as follows:

$$\nu = 1/2 - (E_s/E)(1/2 - \nu_e) \quad (21)$$

$$k_x = .702 (1 - \nu_e^2)^{\frac{1}{2}} Z \quad (22)$$

where Z is a cylinder curvature parameter defined in Ref. 6 as

$$Z = L^2/(Rh) \quad (23)$$

For an isotropic cylinder,

$$\sigma_{cr} = N_x/h \quad (24)$$

$$I = (h^3/12)$$

Upon substitution of Equations (20) through (24) in (19) and using 0.3 for the elastic value of Poisson's ratio, the following equation is obtained for buckling stress

$$\sigma_{cr} = .551 \left\{ E[(E_s/E)(E_t/E)]^{\frac{1}{2}}/(1 - \nu^2) \right\} (h/R) \quad (25)$$

Equation (25) gives the axisymmetric buckling stress for a cylinder as a function of material properties and cylinder geometry.

It is noted that in the elastic stress range Equation (21) reduces to the elastic value for Poisson's ratio, and the corresponding equation for the elastic buckling stress is from Equation (25)

$$\sigma_{c r e} = .605 E (h/R) \quad (26)$$

This is the classical equation for the theoretical local elastic buckling stress for a cylinder.

In order to facilitate the determination of the cylinder geometry ratio (R/h) corresponding to a given buckling stress, it is convenient to rewrite Equation (25) in the following form

$$R/h = .551 \left\{ [(E_s/E)(E_t/E)]^{\frac{1}{2}}/(1 - \nu^2) \right\} (E/\sigma_{cr}) \quad (27)$$

For a given value of the buckling stress, the right hand side of Equations (21) and (27) is a function of material properties only and is determined from an appropriate material stress-strain curve. Hence, a curve of cylinder geometry ratio vs buckling stress can be determined by 1) assuming a value for critical buckling stress, 2) calculating Poisson's ratio from Equation (21) using the material properties for the assumed buckling stress as obtained from a stress-strain curve, and 3) evaluating R/h from Equation (27).

As shown in Ref. 6, the theoretical equation for the axisymmetric buckling stress as given by Equation (25) is in excellent agreement with experimental results when the buckling stress ratio is less than 0.3. This ratio is determined by dividing the buckling stress by a fictitious elastic buckling stress based on the same R/h . From Equations (25) and (26) the buckling stress ratio is thus

$$\sigma_{cr}/\sigma_{cr_e} = .91 [(E_s/E)(E_t/E)]^{1/2}/(1 - \nu^2) \quad (28)$$

Hence, Equations (25) and (27) give accurate estimates of axisymmetric buckling stress and associated cylinder geometry providing

$$\sigma_{cr}/\sigma_{cr_e} < 0.3 \quad (29)$$

To illustrate the application of the equations presented, Figure 6 has been prepared to show possible cylinder designs using 7075-T6 aluminum. The curve of buckling stress ratio vs cylinder geometry was obtained using the procedure outlined above and Equations (21) and (27). Also shown in this figure is a curve of buckling stress ratio vs cylinder geometry and was obtained using Equation (28). Material properties appearing in the equations were evaluated using stress-strain curves presented in Ref. 10. Based on the criterion of Equation (29), it is apparent that 7075-T6 aluminum cylinders designed for axisymmetric buckling should have R/h values less than 25.5; the corresponding buckling stress is 75,000 psi or greater.

The stress for primary column instability of a cylinder as found by the substitution $\rho = R/\sqrt{2}$ (the radius of gyration for a thin walled cylinder) in Equation (9) and rearranging terms is

$$\sigma_c = 4.93 \{ E(E_t/E) \} (R/L)^2 \quad (30)$$

From Equation (30) the cylinder geometry parameter is related to stress and material parameters as follows

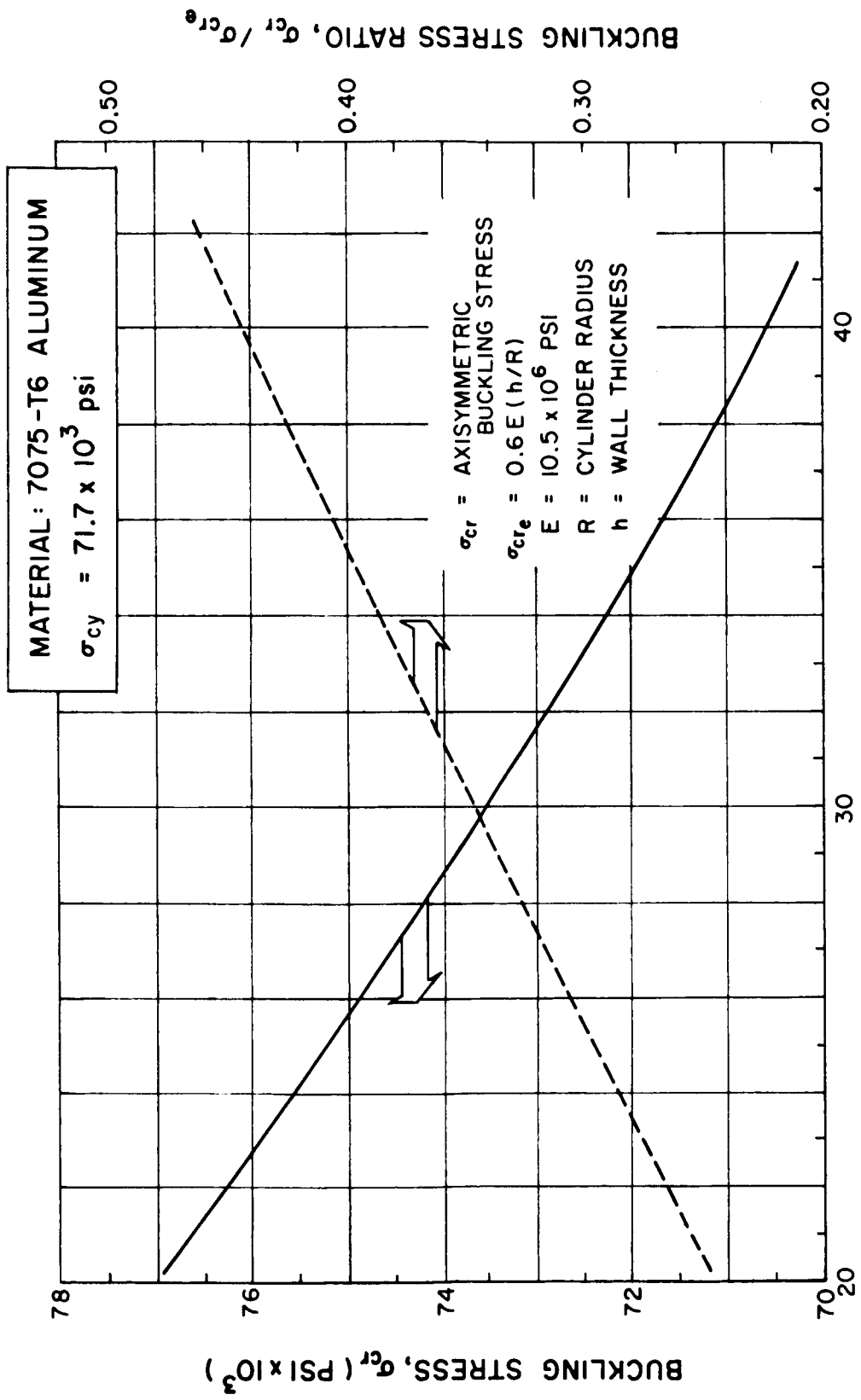


FIG. 6
 CYLINDER GEOMETRY RATIO, R/h

AXISYMMETRIC BUCKLING STRESS VERSUS CYLINDER GEOMETRY

$$(L/R)^2 = 4.93 (E/\sigma_c)(E_t/E) \quad (31)$$

For a given value of buckling stress, the material properties can be determined from stress-strain relationships. Hence, the right hand side of Equation (31) is readily established for a given stress and allows the determination of the corresponding length to radius ratio. For minimum weight, the cylinder should be designed such that the axisymmetric buckling stress and the column instability stress are equal. The optimum length to radius ratio, therefore, is determined using the axisymmetric buckling stress in Equation (31).

The load carried by each strut of the landing system is given by Equation (14) which when expanded in terms of cylinder cross section parameters gives

$$P = n_o W_v / N = \sigma_c 2\pi (R/h) h^2 \quad (32)$$

Equation (32) when solved for h^2 gives

$$h^2 = (n_o W_v / N) [\sigma_c 2\pi (R/h)]^{-1} \quad (33)$$

As indicated, the cylinder wall thickness is a function of the peak deceleration factor, vehicle gross weight, number of struts, design column buckling stress, and cylinder radius to thickness ratio. The optimum peak deceleration factor is determined from considerations presented in a previous subsection. The cylinder radius/wall thickness ratio is determined by axisymmetric buckling considerations as outlined above. For optimum design, the design column buckling stress equals the axisymmetric buckling stress. With this information one can obtain the cylinder wall thickness by means of Equation (33).

The procedure for the design of a deceleration limiter energy absorber is summarized as follows: For a given material of construction, the radius to wall thickness ratio is determined by axisymmetric buckling considerations from curves similar to Figure 6 and the criterion of Equation (29). The optimum length to radius ratio is then determined by column buckling considerations (Eq. 31) with the stipulation that the column buckling stress and the axisymmetric buckling stress are equal. The optimum design peak deceleration factor is determined from considerations presented previously. Finally, the tube wall thickness is found through use of Equation (33). Once the wall thickness is known, the tube radius and length follow directly from the radius to thickness ratio and the length to radius ratio, respectively.

Onset Limiter Configuration

The onset limiting function for the landing system is provided by a structure designed to deform at the yield strength of the material. Control over the onset rate is obtained by shaping the cross sectional area of the structure so that the load resisting vehicle motion is developed gradually.

For a given onset rate and material of construction, the configuration is established by the distribution of cross sectional area. One logical geometric configuration for an onset limiter is the thin walled cone. For this application, consideration of the design radius to wall thickness is necessary to preclude local buckling of the shell as the onset limiter deforms.

The distribution of cross sectional area for an onset limiter follows from consideration of the stroke-time and area-time (for a constant stress) relationships implied by Figure 1. As shown in Figure 1, the vehicle deceleration induced by the onset limiter is assumed to increase linearly with time. Thus the onset rate is constant and the peak deceleration is given by the following equation

$$n_o = \ddot{\bar{x}} t_1 \quad (34)$$

By performing a double integration of the deceleration time history as shown by the onset limiter region of Figure 1 and subject to the conditions that the initial velocity is V_1 and the initial stroke is zero, one obtains the following stroke relationship (see Ref. 2).

$$x = V_1 t_1 (t/t_1) - (\ddot{\bar{x}} g/6)(t_1^3)(t/t_1)^3 \quad (35)$$

Substitution of Equation (34) in (35) and rearranging terms gives

$$x = \left\{ V_1^2/n_o g \right\} \left[\lambda(t/t_1) - (\lambda^2/6)(t/t_1)^3 \right] \quad (36)$$

A nondimensional form of Equation (36) is obtained by dividing both sides of the equation by Equation (2). Thus,

$$\bar{x} = x/x_g = [\lambda(t/t_1) - (\lambda^2/6)(t/t_1)^3]/(\lambda - \lambda^2/6) \quad (37)$$

By Newton's law the force generated by the onset limiter in resistance to vehicle motion consistent with the deceleration history of Figure 1 will also increase linearly with time. If it is further assumed that the onset limiter absorbs landing energy while working to a constant stress level, the cross sectional area of the

energy absorber must increase linearly with time as shown by the following equation

$$\bar{A} = A/A_1 = t/t_1 \quad (38)$$

where A_1 is the maximum cross sectional area and corresponds to time t_1 . Upon substitution of Equation (38) in (37) one obtains

$$\bar{x} = [\lambda \bar{A} - (\lambda^2/6) \bar{A}^3]/(\lambda - \lambda^2/6) \quad (39)$$

Equation (39) gives onset limiter stroke as a function of the cross sectional area and the design parameter λ .

The onset limiter area-stroke equation (Eq. 39) may be further generalized by relating λ to the design parameter β as given by Equation (4). This relationship as determined from Equation (4) is shown by the curve of Figure 7. It is noted that $\lambda = 2.0$ ($\beta = 1.5$) corresponds to energy absorption by means of an onset limiter only, and $\lambda = 0$ ($\beta = 0$) represents energy absorption via a deceleration limiter only.

Figure 8 shows the distribution of onset limiter cross sectional area as a function of stroke and the design parameter β . This curve was determined from Equation (39) and the β vs λ relationship shown in Figure 7. One observes from Figure 8 that the cross sectional area increases as the stroke increases. Also, for a given stroke, the relative area (\bar{A}) increases as β decreases. As noted previously, the physical significance of $\beta = 1.5$ is that the total landing energy is absorbed by the onset limiter. As β decreases, the amount of total landing energy absorbed by the onset limiter decreases. For example, the energy absorbed by the onset limiter for $\beta = 1.1$, 0.8 and 0.4 is 80%, 54%, and 9% of the total landing energy respectively.

The maximum cross sectional area for the onset limiter is determined by equating the load carried by a landing system strut to the maximum deceleration force and results in the following equation

$$A_1 = n_o W_v / (N\sigma) \quad (40)$$

The maximum onset limiter stroke corresponding to this area is given by Equation (2) which for completeness is presented below

$$x_g = (V_1^2/n_o g)[\lambda - \lambda^2/6] \quad (41)$$

In summary, the distribution of the onset limiter cross sectional area as a function of stroke for any value of the design parameter β can be determined from

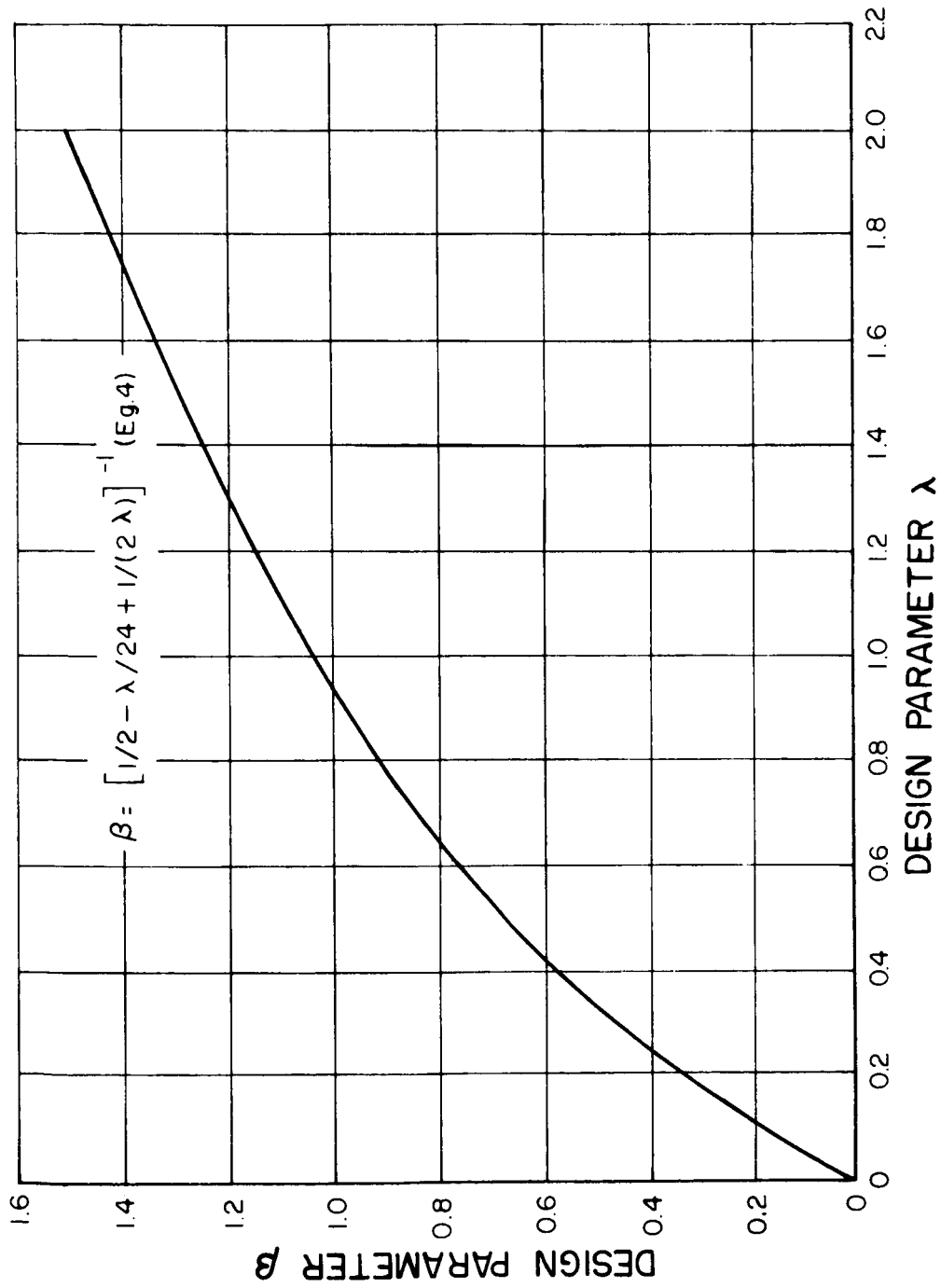


FIG. 7

CURVE OF FUNCTIONAL RELATIONSHIP BETWEEN TWO LANDING SYSTEM DESIGN PARAMETERS

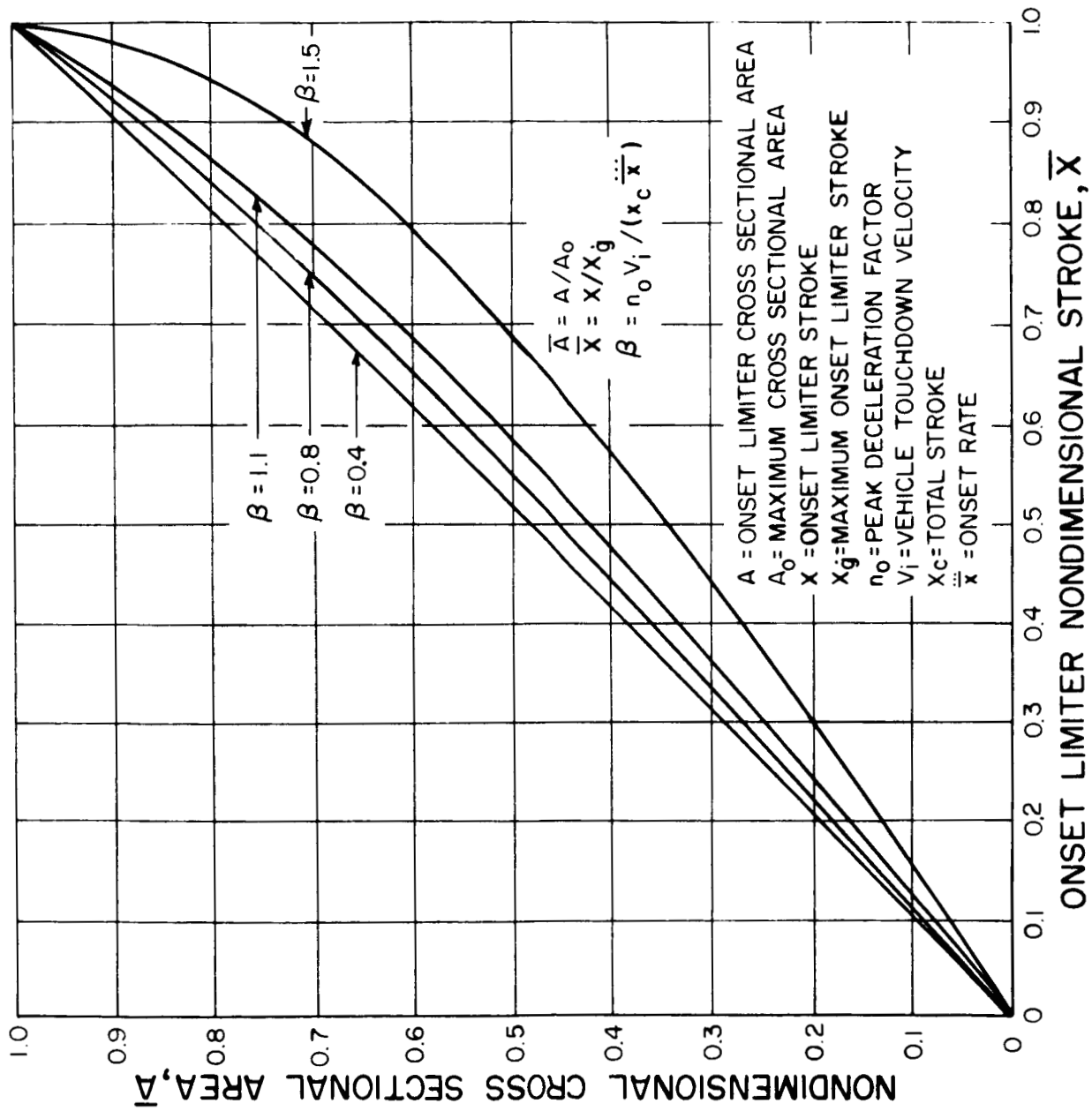


FIG. 8

ONSET LIMITER CROSS SECTIONAL AREA vs STROKE

curves similar to that of Figure 8 together with Equations (40) and (41) and Figure 7. The peak deceleration factor which appears in Equations (40) and (41) is determined from considerations presented in a previous subsection.

One logical configuration for an onset limiter is a thin walled cone. From simple geometric consideration, it can be shown that the thickness distribution for a thin walled cone is given by

$$\bar{h} = h/h_0 = \bar{A}/x \quad (42)$$

where \bar{x} is measured from the cone apex. This equation shows that the thickness distribution can be determined once the nondimensional area vs stroke relationship (such as given by Fig. 8) is known. It is noted that a singular point for Equation (42) occurs when both the area and stroke are zero. For this particular application, the curves of area vs stroke are linear in the region near $x = 0$. (See Fig. 8). Hence, the thickness distribution corresponding to $\bar{x} = 0$ may be found by evaluating the slope ($d\bar{A}/d\bar{x}$) at this point. Based on the above and using Equation (39), one obtains

$$(\bar{h})_{\bar{x}=0} = (d\bar{A}/d\bar{x})_{\bar{x}=0} = (6 - \lambda)/6 \quad (43)$$

With the aid of Equations (42), (43), and Figure 7, the nondimensional area-stroke curves given in Figure 8 were transformed to curves of nondimensional cone wall thickness versus stroke and are shown in Figure 9. One observes from Figure 9 that for a given stroke the relative cone wall thickness increases as the energy absorbed by the onset limiter decreases -- i.e., as β decreases.

The maximum cross sectional area for a thin walled cone is simply

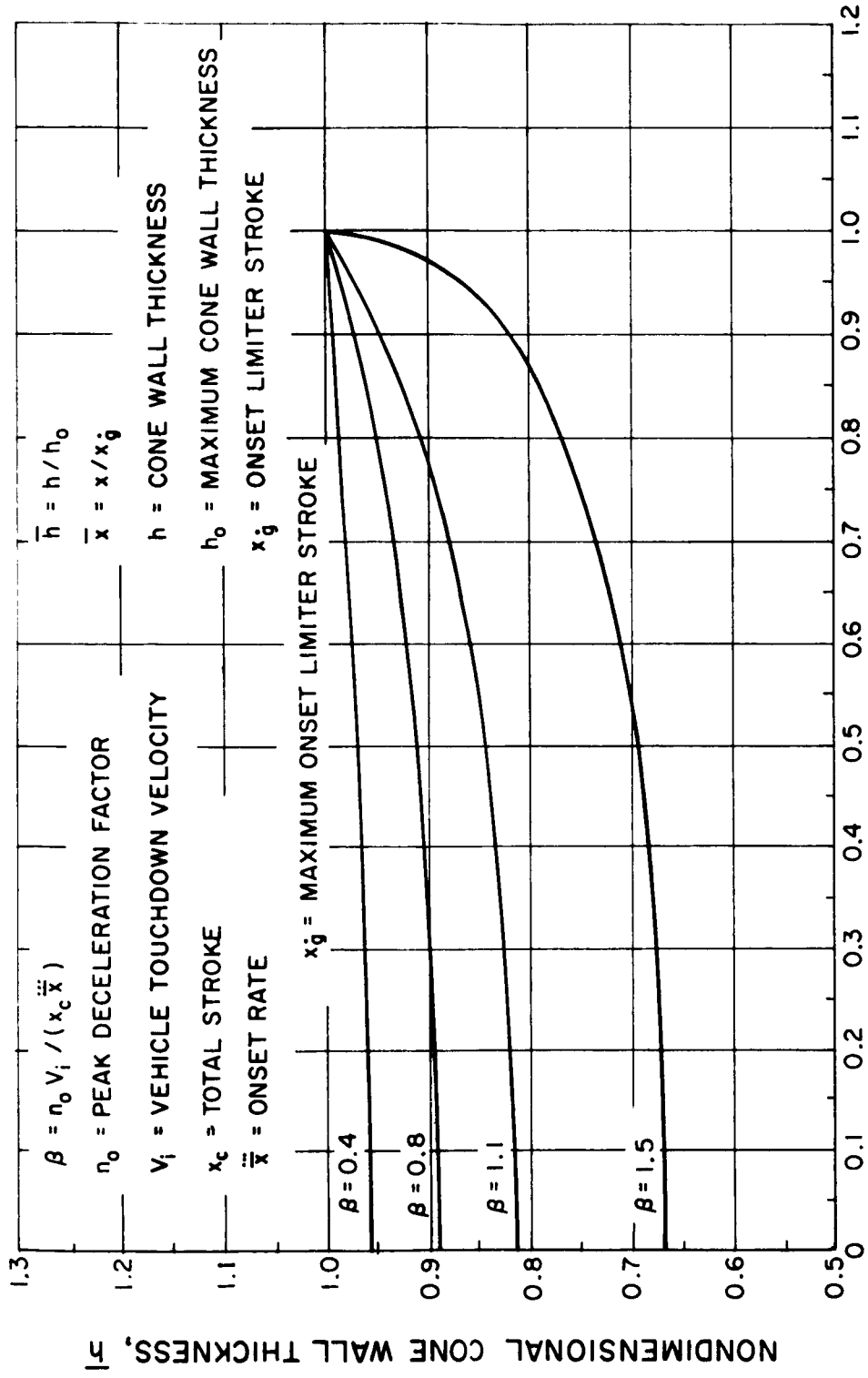
$$A_1 = 2\pi R_0 h_0 \quad (44)$$

Substitution of Equation (44) in (40) allows the maximum thickness to be related to cone geometry and vehicle design parameters as follows

$$h_0^2 = (n_0 W_v / N\sigma) / (2\pi R_0 / h_0) \quad (45)$$

As shown the maximum wall thickness is a function of the base radius to thickness ratio. Limitations on this ratio follow from buckling considerations and are discussed below.

The equations governing onset limiter behavior as presented above are based on the assumption that the material of construction will flow plastically at the design



ONSET LIMITER NONDIMENSIONAL STROKE, \bar{x}

FIG. 9

ONSET LIMITER CONE WALL THICKNESS VERSUS STROKE

stress. This behavior can only be realized for working stresses approaching the yield stress of the material. Other modes of material deformation such as that associated with local buckling of the cone must be suppressed by the choice of design configuration.

Design information pertaining to the asymmetric buckling of a cone subject to axial loading is presented in Ref. 11. As shown in this reference, the elastic buckling stress for a cone is

$$\sigma_{cr} = CE(h/r) \cos \alpha \quad (46)$$

Experimental results presented in Ref. 11 and reproduced herein as Figure 10 shows that the buckling coefficient (C) for cones is the same as that for cylinders providing the equivalent cone radius to thickness ratio is as defined in the figure. Because of the agreement between the buckling behavior of cylinders and cones in the elastic range, it was suggested in Ref. 11 that inelastic behavior for cylinders could be used to predict cone inelastic buckling. With this in mind, Equation (46) is rewritten in the following form

$$\sigma_{cr} = \eta CE(h/r) \cos \alpha \quad (47)$$

where η is a plasticity reduction factor. As shown in Ref. 6 a conservative value of the plasticity reduction factor for cylinders is given by Equation (20).

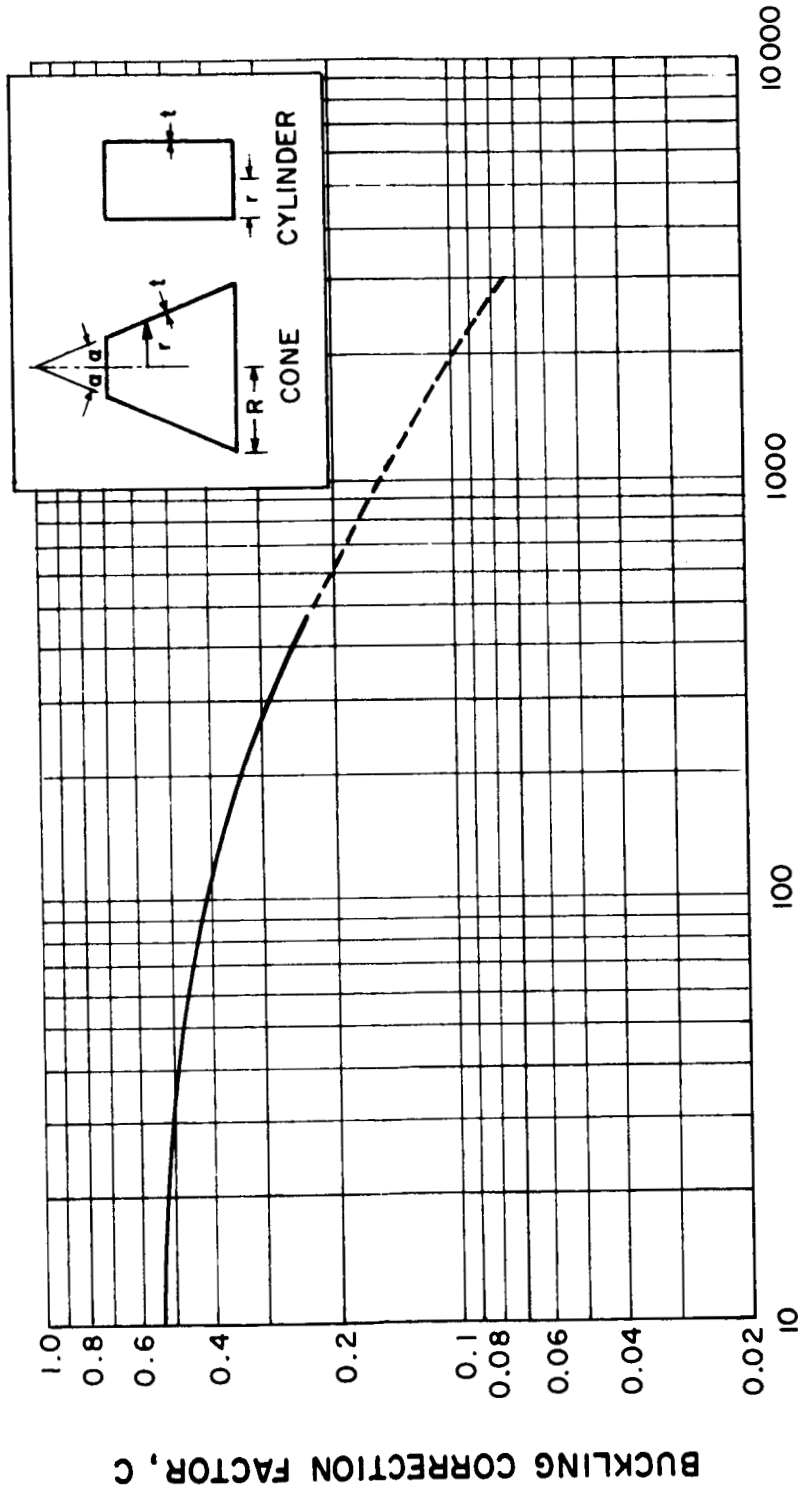
Cone geometry associated with a given buckling stress can be determined by arranging Equation (47) as follows

$$\sigma_{cr}/(\eta E) = C(h/r) \cos \alpha \quad (48)$$

The left hand side of Equation (48) is a function of material properties only and for a given stress and material can be evaluated using Equation (20) and material stress-strain curves.

To illustrate the results of the procedure outlined above, Figure 11 was prepared which shows the cone geometry parameter vs buckling stress for 7075-T6 aluminum material. The material properties used to obtain this curve were from Ref. 10. One observes from Figure 11 that for a buckling stress to yield stress ratio greater than one the cone geometry parameter should be greater than 17.0×10^{-3} .

For a given design and material, the yield stress, design stress, thickness distribution, cone apex angle and radius distribution are known. Also, the buckling



$$r/t \text{ (CYLINDER)} = R/(t \cos \alpha) \text{ (CONE)}$$

FIG.10

BUCKLING CORRECTION FACTOR, C, FOR CYLINDERS OR CONES

(REF.11)

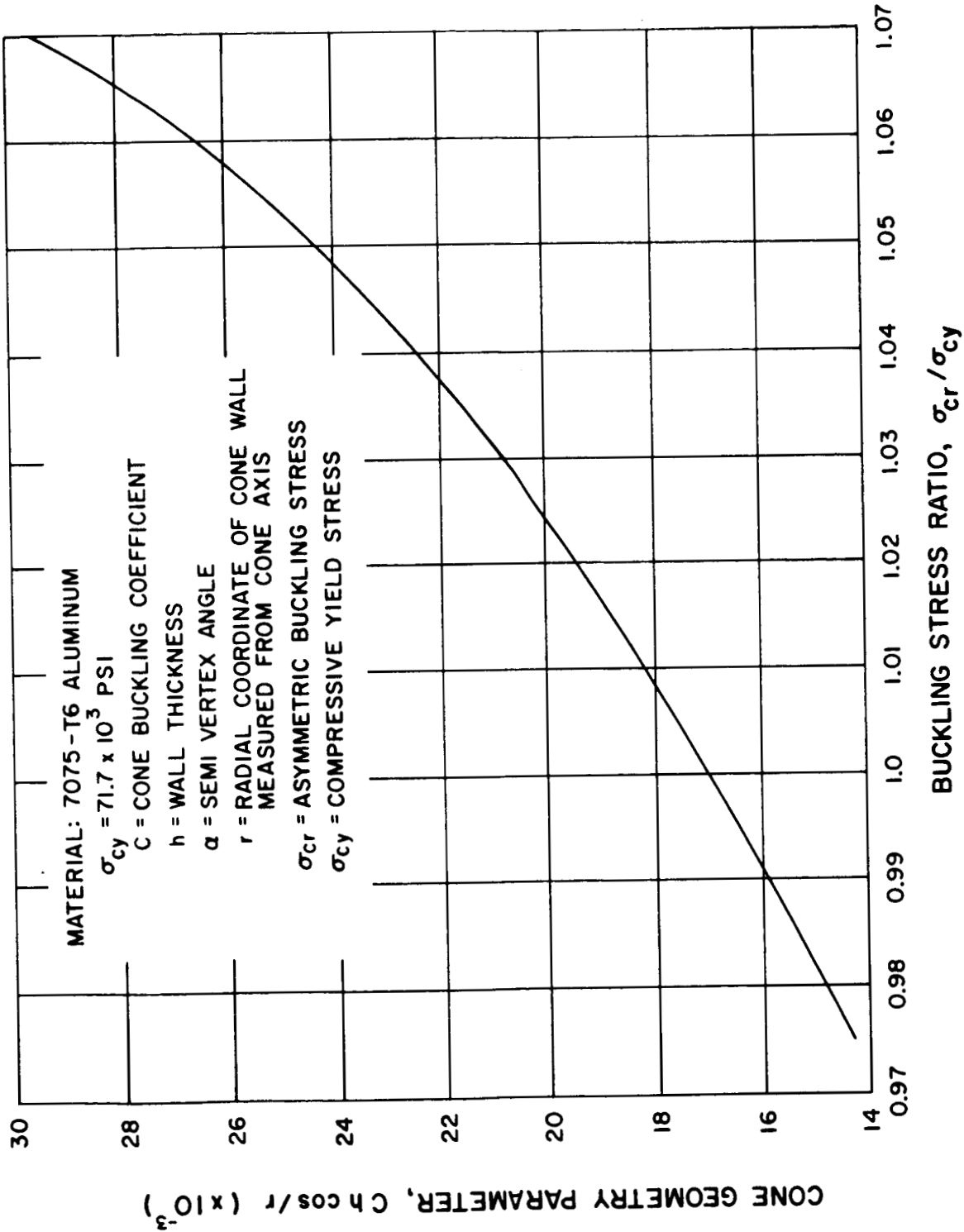


FIG. 11
CONE BUCKLING STRESS VS GEOMETRY

parameter C can be evaluated using Figure 10. The cone geometry parameter $(C h \cos \alpha / r)$ can therefore be evaluated at each cross section and the corresponding value of σ_{cr} / σ_y determined from curves similar to Figure 11. For a design which precludes buckling, it is apparent that

$$\sigma_{cr} / \sigma_y > \sigma / \sigma_y \quad (49)$$

In general, the minimum value for the cone geometry parameter and the corresponding minimum buckling stress will occur near or at the base cross section since at this location "r" is a maximum and "C" is a minimum.

To summarize, the thickness distribution for a thin walled cone which functions as an onset limiter would be determined from curves similar to Figure 9 and Equation (45). The peak deceleration factor would be determined from considerations given in a previous subsection, and the design stress would be chosen approximately equal to the material yield stress. Finally, a cone base geometry would be selected such that the cone buckling stress, as determined from the cone geometry parameter and curves similar to Figure 11, would exceed the onset limiter design stress.

3. DISCUSSION

Two concepts have been proposed for utilizing solid structural materials as efficient energy absorbers. It is suggested that the onset limiting function of a landing system design be realized via a structural element in the form of a tapered shell whose material is designed to flow plastically at the operating stress. The deceleration limiting function would be achieved by a cylindrical shell designed to deform via the axisymmetric buckling mode. It is postulated that these two basic elements, onset limiter and deceleration limiter, when incorporated in a landing system design would provide vehicle deceleration characteristics similar to that of the ideal energy absorber shown in Figure 1.

Considerations necessary to establish the detailed design configuration of energy absorbing elements based on the above concepts have been presented. An analytical method was developed such that the landing system design deceleration factor which corresponds to minimum weight (optimum peak deceleration factor) can be determined once the gross vehicle landing characteristics are defined and the leading parameters for the energy absorption element specified. To illustrate the method a representative curve of optimum peak deceleration was prepared for a particular material of construction (see Fig. 5).

The configuration of the deceleration limiter energy absorbing element was shown to be defined by the radius/wall thickness ratio, length/radius ratio, and wall thickness. These geometric parameters were determined by axisymmetric buckling considerations (Eqs. 27, 28, and 29), column buckling considerations (Eq. 31), and the axial load carried per landing system strut (Eq. 33), respectively.

Curves showing the distribution of cross sectional area for an onset limiter energy absorber were developed in terms of general design parameters (see Fig. 8). For a thin shell design in the form of a cone, the corresponding wall thickness distribution was determined and shown in Figure 9. Since deformation of the onset limiter is predicated on the material of construction flowing plastically at stresses approaching the material yield, it is necessary that the stress associated with buckling deformation modes be greater than the yield stress. For a cone, the stress for the local buckling mode is related to the radius to wall thickness ratio, and limiting values for this ratio for a given material can be determined from Equations (48), (49), and Figure 10.

Although there was some experimental data to substantiate the concept of a controlled onset rate via a structure of tapered cross section (Ref. 7), experimental evidence was not available to support the theory that a cylindrical shell designed

to deform via the axisymmetric buckling mode would provide a constant deceleration type of energy absorber. As part of a limited test program to explore the feasibility of this latter concept, two thin walled cylinders were designed and collapsed under a static load. Figure 12 shows a load-deflection curve faired through the test results. One observes that 1) there is a peak load associated with initial buckling, 2) the strength of the cylinder is approximately 50% of the peak load for most of the stroke, and 3) the working stroke of the cylinder is approximately 80% of its length. The peak collapse load for the cylinders was within 5% of that predicted from theory. Pictures of the collapsed cylinders are shown in Figure 13. Cylinder A of this figure shows the bellows configuration characteristic of the shell at the end of its working stroke. Cylinder B shows a second cylinder at an intermediate stage of deformation.

The results of the cylinder compression tests are significant in that they confirm the hypothesis that the strength of an axisymmetric buckled tube remains essentially constant with stroke thereby providing a capability for deceleration limiting energy absorption. Moreover, the tests indicate that a large portion of the total cylinder length can be developed as working stroke. As in previous investigations (Ref. 6), the peak buckling load was accurately predicted by theory. However, the tests also indicate that the residual strength of a cylinder after initial buckling is considerably less than the peak buckling load. As a result, the theoretical energy absorbing efficiency of the collapsed tube based on the peak collapse load is not realized. The spike in the load-deflection curve would be undesirable in an energy absorbing element because of the associated large decelerations. It would appear, however, that this peak could be eliminated with a negligible loss of working stroke by prebuckling the tubes.

As indicated by the test results, the cylinder residual strength rather than the peak buckling load is the quantity most significant to the energy absorbing capacity of the deceleration limiter element. The development of a theoretical method for predicting the residual strength of a buckled tube would contribute significantly to the implementation of the design concept. In the absence of such theory, it would be necessary to establish an empirical correction factor to the theoretical buckling stress based on the results of a cylinder test program for a given material.

In the development of the analytical method for obtaining both the optimum peak deceleration factor and the deceleration limiter configuration, it was assumed that an optimum design condition could be realized wherein the stress associated

FIG. 12

REPRESENTATIVE LOAD-DEFLECTION CURVE FOR
A CYLINDER DESIGNED TO DEFORM VIA THE
AXISYMMETRIC BUCKLING MODE

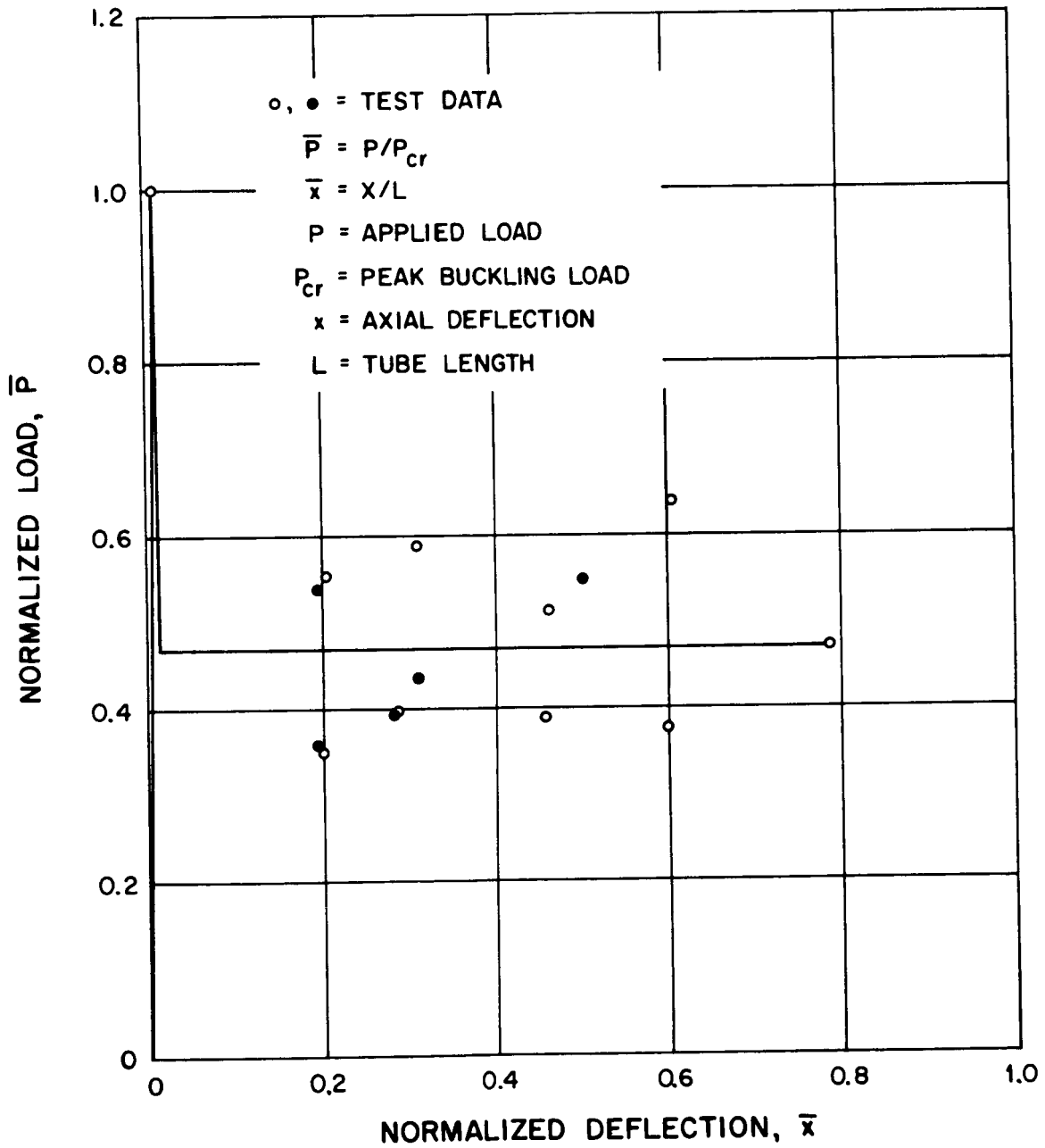


FIG.13

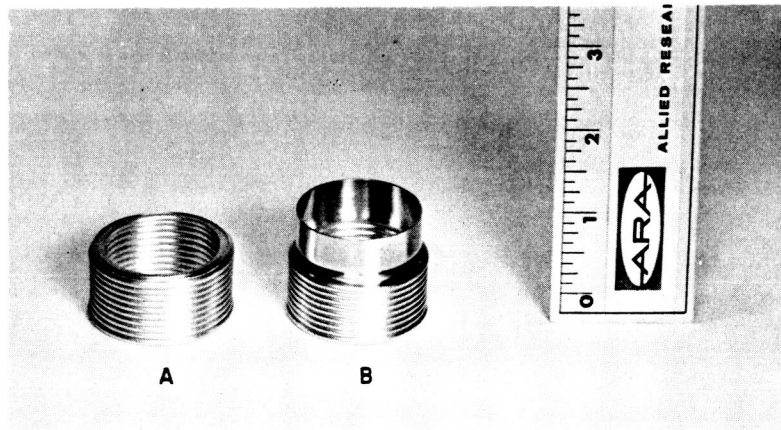
**CYLINDRICAL TEST SPECIMENS
DEFORMED UNDER AXIAL COMPRESSIVE
LOADING VIA AXISYMMETRIC BUCKLING MODE**

Material: 6061-T4

Radius = 0.755 in.

Wall thickness = 0.028 in.

Undeformed Length = 4.0 in.



- A. Cylinder in maximum deformed configuration
- B. Cylinder approaching maximum deformed configuration

with the theoretical axisymmetric buckling and column buckling of the deceleration limiter were equal. The cylinder test results indicate that this optimum stress condition will not be achieved in practice, and that the effective working stress for the cylinder is less than the theoretical buckling stress. As a result, certain modifications are necessary in the design procedure as presented. In essence, the deceleration limiter radius/wall thickness ratio is predicated on the theoretical axisymmetric buckling stress as before, whereas parameters associated with column buckling considerations should be based on the cylinder effective working stress. For example, the cylinder length/radius ratio as given by Equation (31) should be determined using the effective working stress and the associated material properties. In calculating the cylinder wall thickness from Equation (33), one should also use the effective working stress; however, the radius/wall thickness ratio appearing in this equation would still be based on the theoretical axisymmetric buckling stress as previously noted. The changes indicated are based on the assumption that the deceleration limiter would be prebuckled so as to remove the transient peak in the deceleration response. It should be noted that in the fabrication of the energy absorbing element, the cylinder would have to be supported so as to prevent column buckling during the prebuckling operation.

The method presented for determining the optimum peak deceleration factor also involves column buckling considerations and should be modified to account for the difference between the theoretical and effective working stress. In this case, the material and geometry parameter ϕ which appears in the equation for optimum peak deceleration factor (Eq. 18) should be evaluated as follows: The tangent modulus and length/radius ratio should be based on the effective working stress, whereas the radius/wall thickness should be determined by the theoretical axisymmetric buckling stress (see Eq. 13).

As noted in a previous subsection, the method for predicting the optimum deceleration factor is based on the assumption that the deceleration limiter is a more efficient energy absorber than the onset limiter. If the reduction in theoretical efficiency of the deceleration limiter due to its reduced effective working stress result in the onset limiter having the high efficiency, then the optimum peak deceleration factor would simply be the maximum allowable deceleration factor for the payload.

It can be shown that the most efficient energy absorption system is one wherein the onset limiting device absorbs energy at a constant onset rate. Figures 8 and 9

reveal, however, that for a constant onset rate design the onset limiter cross-sectional area is not linear with stroke and becomes increasingly nonlinear as β increases (increasing values of β correspond to a larger fraction of the total energy absorbed by the onset limiter). From manufacturing considerations, it would be desirable to have the cross-sectional area increase linearly with stroke. This latter area distribution would permit an onset limiter cone design, for example, which has a constant wall thickness. In general, the weight and stroke penalty associated with a linear cross-sectional area vs stroke device as compared with a linear cross-sectional area vs time (constant onset rate) device is small. For example, for a design λ of 0.65 and $x/L = 0.8$ wherein the material efficiencies of the onset limiter and deceleration limiter are equal, the total stroke of the linear cross-sectional area vs stroke system is only 6 percent more and the total weight is only 1 percent more than the constant onset rate system.

Additional research is required to define the inelastic buckling stress for cones. In the method presented for checking the cone onset limiter design for local buckling, it was assumed that the plasticity coefficient which gives conservative results for cylinder behavior would also apply for cones. This assumption should be checked experimentally.

An experimental program to evaluate the design procedures developed in this report is warranted. For example, additional static tests should be performed on cylinders as well as thin walled cones to establish their load deflection behavior. Also dynamic tests should be performed on both onset limiter and deceleration limiter elements to establish whether the energy absorbing characteristics of the elements change with the manner in which the load is applied. The dynamic test could be in the form of a simple drop test wherein the motion of a free falling mass is attenuated by the energy absorbing element. Finally, dynamic tests should be performed on the composite system.

4. CONCLUSIONS AND RECOMMENDATIONS

1. Because of the high working stress and large stroke to length ratio associated with the load deflection behavior of a tapered shell which deforms inelastically and a cylindrical shell which deforms via the axisymmetric buckling mode, the combined system provides optimum energy absorption efficiency.
2. Analytical techniques presented in this report allow the optimum design of energy absorbing elements based on the above concepts for the control of the onset rate and maximum deceleration of landing vehicles.
3. Test results on cylinders which buckle in the axisymmetric mode indicate that the force resisting cylinder deformation is essentially constant with stroke and that the working stroke to length ratio is large. These results support the hypothesis that the axisymmetric buckled tube provides efficient energy absorption of the deceleration limiter type.
4. The manufacture of an onset limiter could be facilitated at a relatively small weight and stroke penalty by distributing the cross-sectional area such that the element gives a linear resisting force vs stroke rather than force vs time response.
5. In order to accurately predict the energy absorbing capacity of tubes which deform in the axisymmetric buckling mode, additional information is required concerning the relationship between the peak buckling load and the cylinder residual strength. Such data could be obtained via an experimental program for a particular material of construction.
6. In order to facilitate the design of tapered thin wall shells for energy absorbing structures of the onset limiter type, additional information is desirable concerning inelastic buckling of cones.
7. A comprehensive test program should be initiated to investigate under both static and dynamic loads the energy absorbing characteristics of cylinders which buckle in the axisymmetric mode and cones which deform plastically.

REFERENCES

1. Esgar, J. B., Survey of Energy-Absorption Devices for Soft Landing of Space Vehicles, NASA TN D-1308, June 1962.
2. Milligan, R., and Gerard, G., Weight and Performance Design Indices for Idealized Spacecraft Landing Systems, Allied Research Associates Technical Report No. 235-6, March 13, 1964.
3. Coppa, A. P., Collapsible Shell Structures for Lunar Landings, ARS Paper 2156-61.
4. Fisher, L. J., Jr., Landing Energy Dissipation for Manned Re-entry Vehicles, NASA TN D-453, 1960.
5. McGehee, J. R., A Preliminary Experimental Investigation of an Energy-Absorption Process Employing Frangible Metal Tubing, NASA TN D-1477, October 1962.
6. Gerard, G., "Compressive Stability of Orthotropic Cylinders," Jour. Aero. Sci., Vol. 29, No. 10, October 1962, pp. 1171-1180.
7. Brooks, G. W. and Carden, H. D., "A Versatile Drop Test Procedure for the Simulation of Impact Environments," Shock, Vibration and Associated Environments, Part IV, Bulletin No. 29, June 1961.
8. Gerard, G., and Becker, H., Handbook of Structural Stability Part III - Buckling of Curved Plates and Shells, NACA TN 3783, August 1957.
9. Niles, A. S., and Newell, J. S., Airplane Structures, Vol. I, Third Edition, John Wiley and Sons, Inc., New York, 1949.
10. Mathauser, E. E., Compressive Stress-Strain Properties of 7075-T6 Aluminum-Alloy Sheet at Elevated Temperatures, NACA TN 3854, November 1956.
11. Lackman, L., and Penzien, J., "Buckling of Circular Cones Under Axial Compression," Journal of Applied Mechanics, Vol. 27, Series E, No. 3 September 1960, pp. 458-460.